DALTON
FULL PAPER

An investigation into the photochemical reactions of $MCp(CO)_4$ ($Cp = \eta^5\text{-}C_5H_5$) and $M(\eta^5\text{-}C_9H_7)(CO)_4$ ($\eta^5\text{-}C_9H_7$ = indenyl; M = Nb or Ta) with CO, H_2 and N_2 in solution at room temperature

Gavin I. Childs,[a] David C. Grills,[a] Skip Gallagher,[b] Thomas E. Bitterwolf[b] and Michael W. George *[a]

[a] *School of Chemistry, University of Nottingham, University Park, Nottingham, UK NG7 2RD. E-mail: Mike.George@nottingham.ac.uk*
[b] *Department of Chemistry, University of Idaho, Moscow, ID 83844-2343, USA*

Received 15th December 2000, Accepted 1st March 2001
First published as an Advance Article on the web 15th May 2001

Time resolved step-scan FTIR spectroscopy (s^2-FTIR) has been used to characterise $MCp'(CO)_3L$ (Cp' = Cp or indenyl ($\eta^5\text{-}C_9H_7$); M = Nb or Ta; L = *n*-heptane, H_2 or N_2) in solution at room temperature. $TaCp'(CO)_4$ formed the classical dihydrides, $TaCp'(CO)_3H_2$ upon irradiation in *n*-heptane saturated with H_2. However, photolysis of $Nb(\eta^5\text{-}C_9H_7)(CO)_4$ under the same conditions led to the non-classical complex, $Nb(\eta^5\text{-}C_9H_7)(CO)_3(\eta^2\text{-}H_2)$, whereas irradiation of $NbCp(CO)_4$ resulted in both $NbCp(CO)_3H_2$ and $NbCp(CO)_3(\eta^2\text{-}H_2)$. Photolysis of $MCp'(CO)_4$ in *n*-heptane saturated with N_2 resulted in formation of $MCp'(CO)_3(N_2)$ in all cases. No evidence for disubstitution of these complexes was obtained in these s^2-FTIR experiments. The rate constants for the reaction of $M(\eta^5\text{-}C_9H_7)(CO)_3(n\text{-}C_7H_{16})$ with CO, H_2 and N_2 have been determined. Comparison of these rate constants with those obtained for the analogous cyclopentadienyl complexes showed that the indenyl complexes are more reactive (*ca.* 10 times). Additionally, the $Nb(\eta^5\text{-}C_9H_7)(CO)_3(L)$ (L = $\eta^2\text{-}H_2$ or N_2) complexes were found to be less stable (*ca.* 20–30 times) than $NbCp(CO)_3(L)$, and $Ta(\eta^5\text{-}C_9H_7)(CO)_3(N_2)$ was more reactive (*ca.* 25 times) than $TaCp(CO)_3(N_2)$.

Introduction

Reactions between transition metal complexes and gases are a recurrent feature of organometallic chemistry, particularly in catalytic processes. Hence, transition metal dihydride and dihydrogen complexes are of fundamental interest due to the important role they play as intermediates in these processes.[1–3] Transition metal dihydrides have a long history whereas the first isolable dihydrogen complex was only reported in 1984.[4] The coordination of dinitrogen to transition metals is also of interest because of its relevance to nitrogen fixation.[5,6]

A variety of spectroscopic methods have been used to characterise unstable dihydrogen and dinitrogen complexes. These include the use of frozen gas matrices,[7–11] liquid xenon doped with hydrogen or nitrogen[12–15] and supercritical fluids.[16,17] Time-resolved infrared spectroscopy (TRIR), a combination of flash photolysis and infrared detection, has also been a useful technique for the characterisation of unstable organometallic dihydrogen and dinitrogen complexes at room temperature in solution.[18–20] This technique has the additional advantage of being able to probe reaction kinetics, meaning that the formation and reactivity of unstable dihydrogen and dinitrogen complexes can be monitored.

The formation of organometallic dinitrogen and dihydrogen/dihydride complexes from the photolysis of metal carbonyls in solution usually proceeds *via* a solvated intermediate,† eqn. (1).

$$L_mM(CO)_n \xrightarrow[h\nu]{-CO} [L_mM(CO)_{n-1}] \xrightarrow[\text{fast}]{\text{solvent}} L_mM(CO)_{n-1}(\text{solvent}) \xrightarrow{X_2} L_mM(CO)_{n-1}(X_2) \quad (1)$$

† The only exception to this found, thus far, is a report[21] by Moore and co-workers in which CoCp(CO) appeared not to have any significant interaction with cyclohexane following its generation by flash photolysis of $CoCp(CO)_2$.

The production of these solvated intermediates in alkane solvents has proved to be a convenient route for the formation of alkane complexes which are of interest due to their proposed intermediacy in C–H activation reactions.[21,22] Information regarding both the structure and reactivity of alkane complexes is important for a better understanding of the C–H activation process. Recent studies[23–26] have shown that the reactivity of the alkane complexes $M(\eta^5\text{-}C_5R_5)(CO)_2(\text{alkane})$ (R = H, Me or Et; M = Mn or Re), $M(CO)_5(\text{alkane})$ (M = Cr, Mo or W) and $Cr(\eta^6\text{-}C_6R_6)(CO)_2(\text{alkane})$ (R = H, Me or Et) is affected by both the nature of the aryl substituent and the choice of alkane used. Activation parameters derived from variable temperature time-resolved studies[25,26] have suggested that these alkane complexes decay *via* a mainly associative or associative interchange mechanism, with entropic rather than enthalpic factors governing their reactivity.

There have been relatively few investigations concerning the photochemistry of the Group V carbonyl compounds. Nitrogen bound complexes have been observed following the irradiation of $V(\eta^5\text{-}C_5R_5)(CO)_4$ (R = H, Me or Cl), $V(\eta^5\text{-}C_5H_4Me)(CO)_4$ and $V(\eta^5\text{-}C_9H_7)(CO)_4$ ($\eta^5\text{-}C_9H_7$ = indenyl) in frozen nitrogen matrices at 12 K.[27,28] Photolysis of these complexes in inert matrices resulted in the formation of unsaturated CO-loss complexes. Similarly, irradiation of $MCp'(CO)_4$ (M = Nb or Ta; Cp' = Cp or indenyl) in frozen Nujol[29] yielded the unsaturated CO-loss products, $MCp'(CO)_3$ and $MCp'(CO)_2$. These investigations also observed additional photoproducts which were tentatively assigned to the ring-slipped products, where the hapticity of the cyclopentadienyl or indenyl ring has decreased from 5 to 3. However, recent[30] ultrafast infrared studies on $VCp(CO)_4$ have suggested a possible alternative assignment, with an additional band (at 2020 cm^{-1}) observed upon photolysis being attributed to the triplet state of $VCp(CO)_3$.

A combination of spectroscopic studies in liquid xenon at cryogenic temperatures and fast TRIR at room temperature has been used to probe the photochemistry of the Group 5

complexes $MCp(CO)_4$ (M = V, Nb or Ta) in the presence of both dinitrogen and dihydrogen.[31–33] Formation of $MCp(CO)_{4-n}(N_2)_n$ ($n = 1$ or 2 (Nb only)) was observed for the reactions in the presence of dinitrogen. However, the reactions under dihydrogen gave contrasting results. For V the non-classical dihydrogen complex $VCp(CO)_3(\eta^2\text{-}H_2)$ was formed, whereas for Ta the classical dihydride complex $TaCp(CO)_3H_2$ was formed. For Nb both the non-classical $NbCp(CO)_3(\eta^2\text{-}H_2)$, and the classical $NbCp(CO)_3H_2$ complexes were observed; furthermore, these complexes were found to be in rapid equilibrium. At room temperature $VCp(CO)_3(\eta^2\text{-}H_2)$ is not stable, and decays over 40 ms in the presence of 2 atm of hydrogen. $TaCp(CO)_3H_2$ is rather less reactive, with a half-life of 5 minutes in supercritical xenon under 100 atm of hydrogen. TRIR measurements showed that $VCp(CO)_3(n\text{-}C_7H_{16})$ was *ca.* 100 times more reactive towards H_2, N_2 and CO than the corresponding complexes of Nb and Ta. Recently[34] we have described the characterisation of $MCp'(CO)_3(N_2)$ (Cp′ = Cp or indenyl; M = Nb or Ta), $NbCp'(CO)_2(N_2)_2$, $TaCp'(CO)_3H_2$, $Nb(\eta^5\text{-}C_9H_7)(CO)_3(\eta^2\text{-}H_2)$, $NbCp(CO)_3(\eta^2\text{-}H_2)$ and $NbCp(CO)_3H_2$ following irradiation of $MCp'(CO)_4$ (**1**–**4**) in polyethylene (PE) matrices surrounded by reactant gas at low temperature. The use of a PE matrix enabled the investigation of the thermal gas exchange reactions of these unstable complexes. We observed the formation of $TaCp'(CO)_3H_2$ after warming $TaCp'(CO)_3(N_2)$ from 160 to 280 K under a pressure of hydrogen.

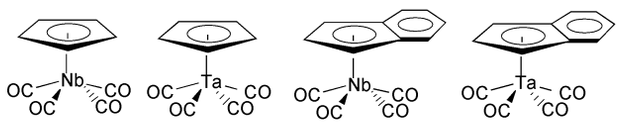

1 **2** **3** **4**

The reactivities of $TaCp(CO)_3H_2$ and $Ta(\eta^5\text{-}C_9H_7)(CO)_3H_2$ in PE discs at room temperature could be measured using conventional FTIR spectroscopy. $Ta(\eta^5\text{-}C_9H_7)(CO)_3H_2$ was *ca.* 50 times more reactive than $TaCp(CO)_3H_2$ in PE at room temperature. The niobium and dinitrogen compounds characterised in our previous study were too reactive to be monitored in PE at room temperature using conventional FTIR spectroscopy.

Recent studies[35] by Ford and co-workers have investigated the photodecarbonylation of $FeCp'(CO)_2(C(O)CH_3)$ (Cp′ = Cp or indenyl) at room temperature using time-resolved techniques. They found that the indenyl intermediate was *ca.* 5 times more reactive towards methyl migration and towards trapping by various ligands than the corresponding Cp analogue. No evidence for production of intermediates with their hapticity changed was observed (*e.g.* η^5 to η^3), and the authors suggest that the fivefold difference in reactivity was not great enough to support a ring-slip mechanism. This should be contrasted to the fact that the reaction of PPh_3 with $RhCp(CO)_2$ is 8 orders of magnitude smaller than for the analogous reaction with $Rh(\eta^5\text{-}C_9H_7)(CO)_2$, suggesting that a ring-slip intermediate plays a major role in the increased reactivity of the indenyl complex.[36]

In this paper we investigate the difference in reactivity between $MCp(CO)_3L$ and $M(\eta^5\text{-}C_9H_7)(CO)_3L$ (M = Nb or Ta; L = *n*-heptane (C_7H_{16}), H_2 or N_2) at room temperature in *n*-heptane. We have used step-scan FTIR (s^2-FTIR) to characterise these unstable species and diode-laser based TRIR to probe the reaction kinetics.

Results and discussion

Characterisation of the reaction products

Compounds **1**–**4** have local C_{4v} symmetry and as such they all exhibit the two expected IR active *ν*(C–O) vibrations (a_1 and e). The IR inactive b_1 stretch, observed in previous[29,34] low temperature studies, was not seen in these room temperature

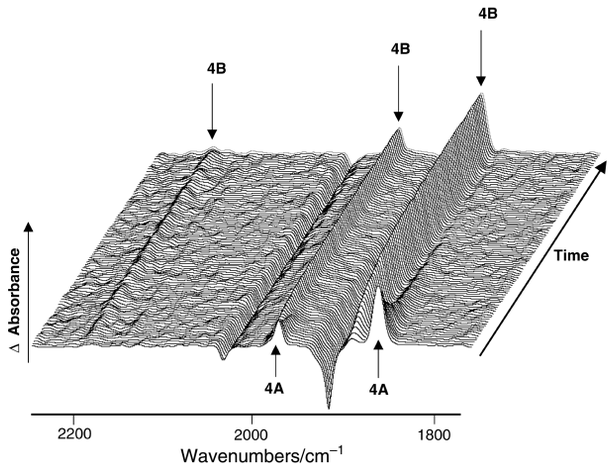

Fig. 1 s^2-FTIR waterfall plot showing the decay of $Ta(\eta^5\text{-}C_9H_7)(CO)_4$ **4** in *n*-heptane saturated with N_2 (2 atm). An initial photoproduct, $Ta(\eta^5\text{-}C_9H_7)(CO)_3(n\text{-}C_7H_{16})$ **4A**, is formed 1 μs after photolysis. This initial photoproduct decays, concurrent with a growth in a secondary product which can be assigned to $Ta(\eta^5\text{-}C_9H_7)(CO)_3(N_2)$ **4B**. FTIR spectra were recorded at 1 μs intervals. Similar results were obtained for **1**–**3**.

solution studies. s^2-FTIR was used to monitor the changes following irradiation of **1**–**4** in *n*-heptane saturated with either N_2 or H_2 (2 atm). We have repeated the characterisation of the photoproducts of **1** and **2,** which have previously been identified at room temperature using the 'point-by-point' laser-based TRIR technique.[33] The photoproducts of **3** and **4** have not previously been characterised at room temperature.

Fig. 1 shows the s^2-FTIR spectra obtained after photolysis (355 nm) of **4** in *n*-heptane saturated with N_2. A decrease in the parent *ν*(C–O) bands is observed, concurrent with the growth of three new bands at wavenumbers lower than those of **4** (the lower of the observed carbonyl stretches contains two unresolved bands). These new bands can be assigned to $Ta(\eta^5\text{-}C_9H_7)(CO)_3(n\text{-}C_7H_{16})$ **4A** by comparison to previous room temperature TRIR studies.[33] Fig. 1 also shows that the bands due to **4A** decay over a period of *ca.* 10 μs, concurrent with a growth in three new carbonyl bands and a characteristic *ν*(NN) band. These new bands can be assigned to $Ta(\eta^5\text{-}C_9H_7)(CO)_3(N_2)$ **4B** by comparison with our low temperature PE matrix results.[34] Comparable results were obtained following irradiation of **1, 2** and **3** in *n*-heptane doped with N_2, with the heptane complexes (**1A, 2A** and **3A**) being formed initially and the dinitrogen substituted complexes (**1B**, **2B** and **3B**) growing in as the *n*-heptane complexes decay. The IR band positions of these complexes are collected in Table 1. No evidence for multiple CO-loss products, as seen in previous low temperature studies,[29,34] was observed. The general scheme for the reactions observed following irradiation of **1**–**4** in *n*-heptane doped with N_2 is shown below.

$$Cp'M(CO)_4 \xrightarrow[n\text{-heptane}]{\text{UV, RT}} Cp'M(CO)_3(n\text{-}C_7H_{16}) \xrightarrow{N_2} Cp'M(CO)_3(N_2)$$

The photolysis of **1**–**4** was repeated in *n*-heptane saturated with H_2 (2 atm). Initially, identical results to those seen under N_2 were observed, with **1A**–**4A** being formed. However, as the *n*-heptane complexes decayed, contrasting results were obtained. Fig. 2 shows the step-scan FTIR spectra obtained *ca.* 25 μs after irradiation of **1**–**4** in *n*-heptane doped with hydrogen. As **2A** and **4A** decay new *ν*(C–O) bands at wavenumbers *higher* than those of the parent species appear. This indicates oxidation of the metal centre, and these stretches can be assigned to formation of the classical dihydride complexes $TaCp(CO)_3H_2$ **2C** and $Ta(\eta^5\text{-}C_9H_7)(CO)_3H_2$ **4C**, which are consistent with previous low temperature[34] and room temperature studies.[33]

Table 1 IR band positions (cm^{-1}) of $MCp'(CO)_{4-x}(L)$ (Cp′ = Cp or indenyl; M = Nb or Ta; $x = 0$ or 1; L = H_2, N_2 or matrix material) species. For the unsaturated compounds the vacant site is filled by coordination of the matrix material or solvent

Compound	PE (Low T)[a]	Xe (203 K)[b]	*n*-Heptane (298 K)[c]	Nujol matrix (77 K)[d]
1 $NbCp(CO)_4$	2035	2038.5	2036.5	2034
	1942.5	1933.5	1931.5	1942
	1927			1927
1A $NbCp(CO)_3$	1980.5		1983.5	1982
	1877.5		1879.5[e]	1881
	1870			1871
1B $NbCp(CO)_3(N_2)$	2191	2193	2195	
	1988	1992.5	1991	
	1898.5[e]	1906[e]	1905[e]	
1D $NbCp(CO)_3(\eta^2\text{-}H_2)$	1995.5	2001[a,b]	2000.5	
	1908	1915[a,b]	1901[e]	
	1894	1902[a,b]		
1C $NbCp(CO)_3H_2$	2049	2053[a,b]	2052	
	2001	2006[a,b]	2006	
	1959	1966[a,b]	1965	
2 $TaCp(CO)_4$	2032.5	2036	2034	2033
	1932	1925.5	1924.5	1934
	1919			1918
2A $TaCp(CO)_3$	1974		1977	1977
	1868		1867[e]	1872
	1860			1859
2B $TaCp(CO)_3(N_2)$	2163	2164	2166	
	1981.5	1986	1985	
	1891.5[e]	1899[e]	1898[e]	
2C $TaCp(CO)_3H_2$	2049	2053.5[b]	2051	
	1996	2002[b]	1999.5	
	1952	1958.5[b]	1956.5	
3 $Nb(\eta^5\text{-}C_9H_7)(CO)_4$	2034		2035	2034
	1947		1931.5	1947
	1929.5			1930
3A $Nb(\eta^5\text{-}C_9H_7)(CO)_3$	1980		1981.5	1980
	1884		1886	1883
	1873.5		1875	1873
3B $Nb(\eta^5\text{-}C_9H_7)(CO)_3(N_2)$	2202		2204	
	1988		1989	
	1905		1905[e]	
	1897			
3D $Nb(\eta^5\text{-}C_9H_7)(CO)_3(\eta^2\text{-}H_2)$	1993.5	1997[a]	1996.5	
	1907.5	1912.5[a]	1910.5	
	1896	1901[a]	1901.5	
4 $Ta(\eta^5\text{-}C_9H_7)(CO)_4$	2031		2033	2032
	1935.5		1924	1937
	1921			1921
4A $Ta(\eta^5\text{-}C_9H_7)(CO)_3$	1973.5		1976	1975
	1871.5		1873[e]	1873
	1865			1864
4B $Ta(\eta^5\text{-}C_9H_7)(CO_3)(N_2)$	2172.5		2174.5	
	1981.5		1984	
	1897		1899[e]	
	1892			
4C $Ta(\eta^5\text{-}C_9H_7)(CO)_3H_2$	2048		2050	
	1996.5		1999.5	
	1954.5		1958	

[a] See reference 34. [b] See reference 33. [c] This study. [d] See reference 30. [e] Unresolved bands.

However, as **3A** decays, the growth of three new carbonyl stretches at band positions *lower* than those of the parent is observed, and therefore these bands can be assigned to the non-classical complex, $Nb(\eta^5\text{-}C_9H_7)(CO)_3(\eta^2\text{-}H_2)$ **3D**. No evidence is seen for formation of the classical dihydride. As **1A** decays, new IR bands due to both the non-classical $NbCp(CO)_3(\eta^2\text{-}H_2)$ and the classical $NbCp(CO)_3H_2$ are observed. These results are consistent with our previous low temperature polymer studies[34] (see Table 1). Formation of a dihydride by third row elements is consistent with results seen for Group 7 and Group 8 compounds.[16,37] Third row complexes have increased back bonding from the metal centre to the coordinated dihydrogen. This results in overpopulation of the unoccupied σ* orbital of the dihydrogen, causing cleavage of the H–H bond and formation of the classical dihydride complex. The increase in coordination number upon formation of a dihydride complex also means that this type of complex is favoured for the third row transition metal complexes. The schemes for the reactions observed following irradiation of **1**–**4** in *n*-heptane doped with H_2 are shown below.

From the s^2-FTIR plots it can also be seen that the *n*-heptane complexes (**1A**–**4A**) decay at the same rate as the corresponding dinitrogen (**1B**–**4B**) and dihydrogen (**1D**, **3D**)/dihydride (**1C**, **2C**, **4C**) complexes grow in, Fig. 3.

Kinetic measurements

To obtain accurate kinetic data for the decay of **1A**–**4A** in *n*-heptane we have measured the decay rates at varying concentrations of CO, H_2 and N_2. The heptane complexes, **1A**–**4A**, decay *via* pseudo-first order kinetics and a plot of the observed rate constant, k_{obs}, against concentration of L (CO, H_2 or N_2)

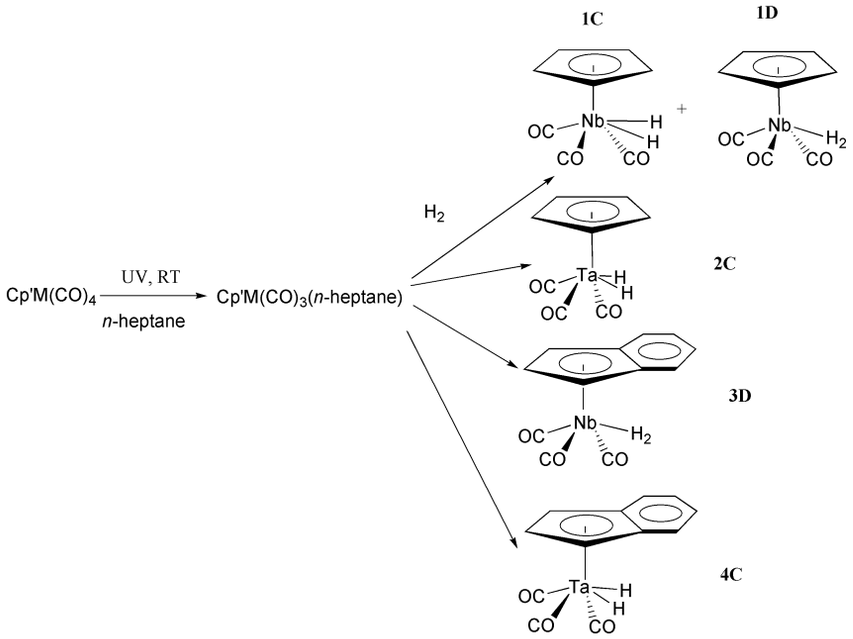

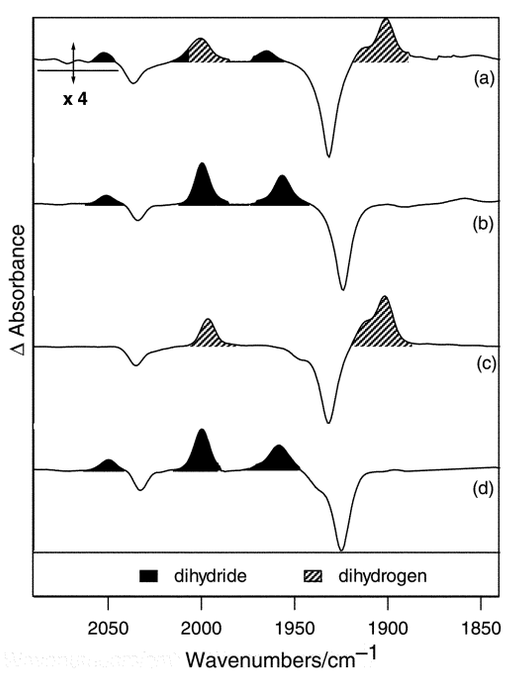

Fig. 2 Step-scan FTIR difference spectra obtained *ca.* 25 μs following UV irradiation of (a) $NbCp(CO)_4$ **1**, (b) $TaCp(CO)_4$ **2**, (c) $Nb(\eta^5\text{-}C_9H_7)(CO)_4$ **3** and (d) $Ta(\eta^5\text{-}C_9H_7)(CO)_4$ **4** in *n*-heptane saturated with H_2 at room temperature. Negative peaks are due to depletion of parent, with positive peaks due to formation of hydrogen bound species.

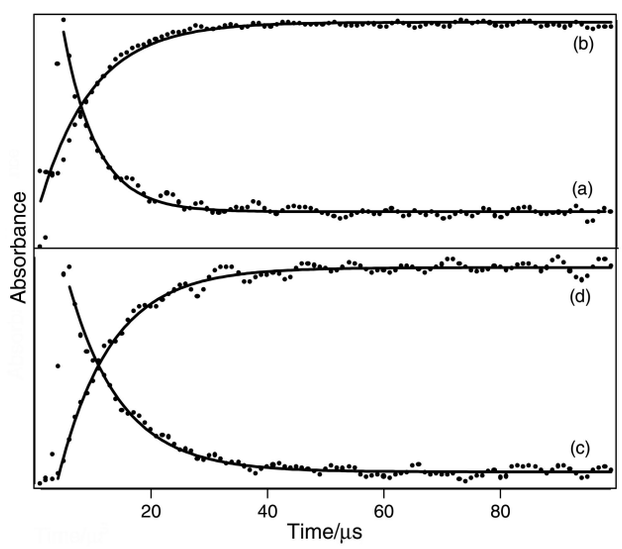

Fig. 3 Plots of absorbance against time obtained from the s^2-FTIR spectra showing (a) the decay of $Nb(\eta^5\text{-}C_9H_7)(CO)_3(n\text{-}C_7H_{16})$ **3A** and (b) the growth of $Nb(\eta^5\text{-}C_9H_7)(CO)_3(N_2)$ **3B** in *n*-heptane doped with N_2. This plot also shows (c) the decay of **3A** and (d) the growth of $Nb(\eta^5\text{-}C_9H_7)(CO)_3(\eta^2\text{-}H_2)$ **3D** in *n*-heptane doped with H_2. These traces have been normalised for ease of viewing. It is clear from these plots that the heptane complexes decay at the same rate as the hydrogen or nitrogen bound complexes grow in. Comparable results were observed for the corresponding Cp complexes and for the tantalum analogues.

yields the second order rate constant for the reaction with the various reactant gases. (Fig. 4). Under increasing pressure of CO, H_2 or N_2 the rate of decay of **1A**–**4A** also increases. From these plots it is clear that the indenyl complexes, **3A** and **4A**, are *ca.* 10 times more reactive than the corresponding Cp complexes, **1A** and **2A**. The second order rate constants obtained from these plots are given in Table 2.

The rate constants obtained for the reaction of $MCp(CO)_3(n\text{-}C_7H_{16})$ with L in this study are slightly lower than those obtained previously.[38] However, the values obtained here still follow the observed trends[39] concerning the reactivity of organometallic *n*-heptane complexes, where a decrease in reactivity is observed upon moving down the Periodic Table and upon moving from Group 5 to Group 7.

We have also monitored the decay of the dihydrogen and dinitrogen complexes. We were unable to measure the decay of the dihydride complexes (**1C, 2C** and **4C**) because these species were too long-lived (lifetime > 10 seconds) to be studied using our diode laser apparatus. Fig. 5 shows the kinetic traces obtained for the decay of the dinitrogen complexes (**1B**–**4B**) and the dihydrogen complexes (**1D** and **3D**). As **1B**–**4B** decay the parent $MCp'(CO)_4$ species (**1**–**4**) are only very slightly regenerated. This may be due to the dinitrogen complexes decaying *via* reaction with parent to form a dimeric species. Similar results were obtained in studies[26] of the Group 7 half-sandwich complexes. The decay of $MCp'(CO)_3(L)$ *via* reaction with parent would be expected to occur *via* pseudo-first order kinetics since the concentration of parent is far greater than that of the dinitrogen complex, and as such we have used an exponential fit for the decay traces. From these plots it is clear that the $M(\eta^5\text{-}C_9H_7)(CO)_3(N_2)$ (**3B** and **4B**) complexes are *ca.* 20–30 times less stable than the $MCp(CO)_3(N_2)$ (**1B** and **2B**) complexes. Similar results are observed for the dihydrogen

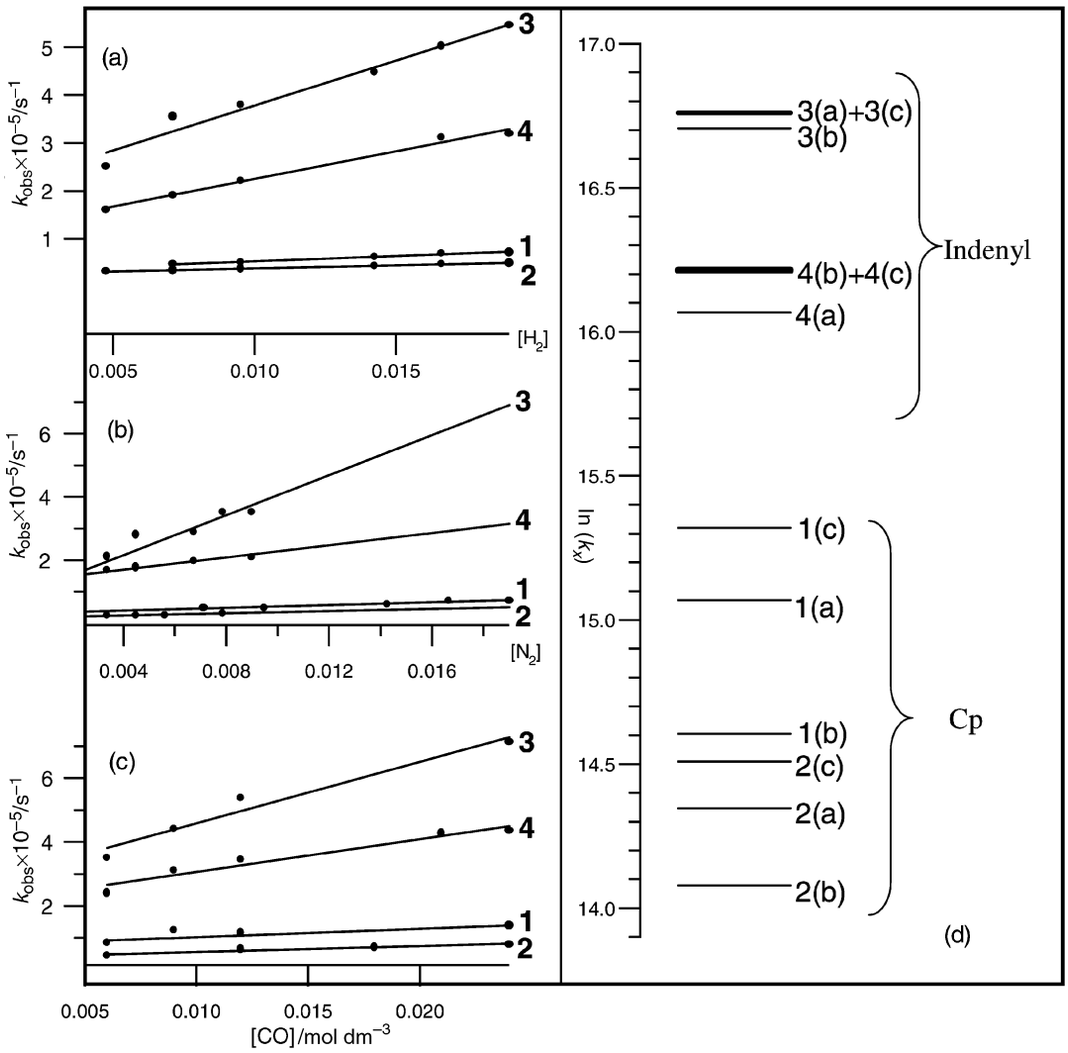

Fig. 4 Plots of observed rate constant, k_{obs}, against [X] (X = (a) H_2, (b) N_2 or (c) CO) for the reaction of $MCp'(CO)_3(n\text{-}C_7H_{16})$ with X. These plots yield the second order rate constant, k_x, for the reaction of **1A**–**4A** with (a) H_2, (b) N_2 or (c) CO. The relative values of k_x are given in Table 2 and shown graphically in (d).

Table 2 Second-order rate constants, k_{CO}, k_{H_2}, and k_{N_2}/dm^3 mol^{-1} s^{-1}, for the reaction of **1A**–**4A** with CO, H_2 and N_2 in *n*-heptane at 298 K

Complex	k_{CO}	k_{H_2}	k_{N_2}
1A $NbCp(CO)_3(n\text{-}C_7H_{16})$	4.5×10^6 [a]	3.5×10^6	2.2×10^6
2A $TaCp(CO)_3(n\text{-}C_7H_{16})$	2.0×10^6 [a]	1.7×10^6	1.3×10^6
3A $Nb(\eta^5\text{-}C_9H_7)(CO)_3(n\text{-}C_7H_{16})$	1.8×10^7	1.9×10^7	1.9×10^7
4A $Ta(\eta^5\text{-}C_9H_7)(CO)_3(n\text{-}C_7H_{16})$	1.1×10^7	9.5×10^6	1.1×10^7

[a] See reference 37.

Table 3 Observed decay constants and lifetimes ($1/k_{obs}$) for the decay of various dinitrogen and dihydrogen complexes at 298 K

Complex	k_{obs}/s^{-1}	Lifetime/s
1B $NbCp(CO)_3(N_2)$	24.2	0.04
2B $TaCp(CO)_3(N_2)$	0.6	1.6
3B $Nb(\eta^5\text{-}C_9H_7)(CO)_3(N_2)$	480	0.002
4B $Ta(\eta^5\text{-}C_9H_7)(CO)_3(N_2)$	17	0.06
1D $NbCp(CO)_3(\eta^2\text{-}H_2)$	15	0.07
3D $Nb(\eta^5\text{-}C_9H_7)(CO)_3(\eta^2\text{-}H_2)$	540	0.002

complexes. The indenyl complex, **3D**, is *ca*. 30 times less stable than its Cp analogue, **1D** (Table 3). In principle a lower ν(NN) frequency is indicative of a stronger M–N_2 bond, which is consistent with the experimental observations. In practice the reactivity of a compound will be influenced by several factors including the mechanism of the reaction.

Although the difference in reactivity between the indenyl and the cyclopentadienyl complexes described in this paper is significant, it is much less dramatic than the difference observed [36] in the reactivities of $RhCp(CO)_2$ and $Rh(\eta^5\text{-}C_9H_7)(CO)_2$ towards PPh_3, where the ring slippage pathway leads to a 10^8 enhancement in the latter case. The differences in the reactivity between the Cp and indenyl complexes described in this paper are larger than those seen by Ford and co-workers in their investigation into the photodecarbonylation of $FeCp(CO)_2(C(O)CH_3)$ and $Fe(\eta^5\text{-}C_9H_7)(CO)_2(C(O)CH_3)$, where only a 5-fold enhancement in rate was observed.

It is interesting that for all the complexes we have studied we are observing similar trends in reactivity for the niobium and tantalum cyclopentadienyl/indenyl systems. For a given *n*-heptane, dihydrogen or dinitrogen complex we find that the indenyl complex is *ca*. 10–30 times more reactive than the corresponding cyclopentadienyl analogue. In previous investigations [23,24] concerning other early transition metal alkane complexes, $Mn(\eta^5\text{-}C_5Me_5)(CO)_2(n\text{-}C_7H_{16})$ was *ca*. 2 times more reactive towards CO, H_2 or N_2 than $MnCp(CO)_2(n\text{-}C_7H_{16})$. Similarly, $Cr(\eta^6\text{-}C_6Me_6)(CO)_2(n\text{-}C_7H_{16})$ had a greater rate constant for the reaction with CO than the corresponding $Cr(\eta^6\text{-}C_6H_6)(CO)_2(n\text{-}C_7H_{16})$ complex. In both these cases the increase in reactivity was largely attributed to steric rather than

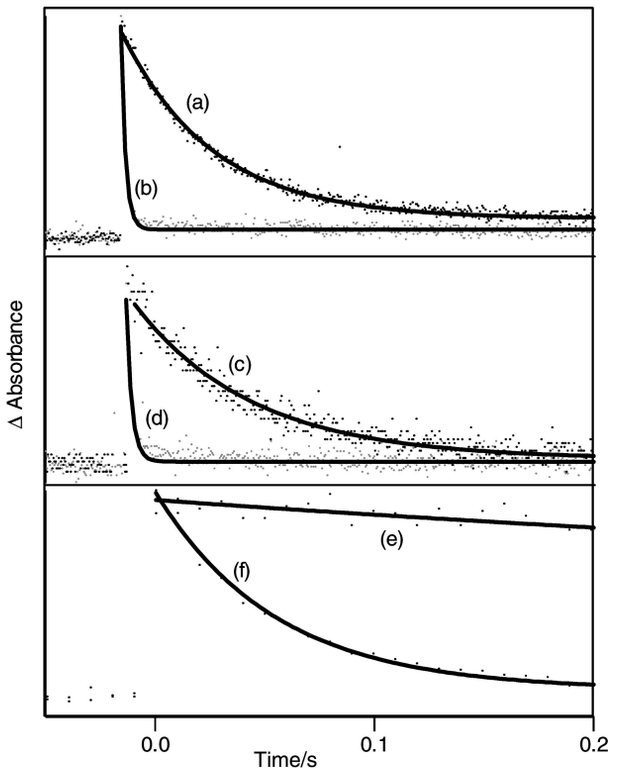

Fig. 5 Kinetic traces comparing the decays of (a) $NbCp(CO)_3(N_2)$ **1B**, (b) $Nb(\eta^5\text{-}C_9H_7)(CO)_3(N_2)$ **3B**, (c) $NbCp(CO)_3(\eta^2\text{-}H_2)$ (**1D**), (d) $Nb(\eta^5\text{-}C_9H_7)(CO)_3(\eta^2\text{-}H_2)$ **3D**, (e) $TaCp(CO)_3(N_2)$ **2B** and (f) $Ta(\eta^5\text{-}C_9H_7)(CO)_3(N_2)$ **4B**. These traces have been normalised for ease of viewing. From these decay traces it is clear that the indenyl complexes are more reactive than their Cp counterparts.

electronic factors. For the complexes investigated in this paper, the rate constants for the reaction of $M(\eta^5\text{-}C_9H_7)(CO)_3(n\text{-}C_7H_{16})$ with CO, H_2 or N_2 are larger than those for the corresponding reactions for $MCp(CO)_3(n\text{-}C_7H_{16})$. The ν(C–O) band positions of **1** and **2** are similar to those of **3** and **4** respectively (see Table 1), indicating that there is a similar electron density on the metal centre in each set of complexes. We have investigated whether the increase in rate for the indenyl substituted complexes is due solely to steric factors by examining the photoreactivity of $Re(\eta^5\text{-}C_5Ph_5)(CO)_2(Solv)$ and $Re(\eta^5\text{-}C_5H_5)(CO)_2(Solv)$ (Solv = alkane or xenon).

Interpretation of differences in rate constants requires careful consideration since the reaction may proceed *via* an associative, associative interchange, dissociative interchange or dissociative mechanism, or a combination of these pathways. Early transition metal alkane complexes are thought to react in alkane solution *via* mainly an associative or associative interchange mechanism.[26] However, for organometallic xenon complexes there is evidence that the reactivity of these complexes has a significant dissociative component.[40,41] We have previously[26] compared the reactivity of $Re(\eta^5\text{-}C_5Ph_5)(CO)_2(\text{cyclo-}C_5H_{10})$ and $Re(\eta^5\text{-}C_5H_5)(CO)_2(\text{cyclo-}C_5H_{10})$ at low temperature, observing that the phenyl substituted complex is *ca*. 6 times more reactive towards CO than the non-substituted complex. Similarly, we have observed[42] that $Re(\eta^5\text{-}C_5Ph_5)(CO)_2(Xe)$ ($k_{CO} = 2.4 \times 10^4$ dm^3 mol^{-1} s^{-1}) is *ca*. 5 times more reactive than $Re(\eta^5\text{-}C_5H_5)(CO)_2(Xe)$ ($k_{CO} = 4.8 \times 10^3$ dm^3 mol^{-1} s^{-1}). Regardless of the mechanism by which the complexes described in this paper decay, comparison of the results presented with the $Re(\eta^5\text{-}C_5H_5)(CO)_2(Solv)$ (Solv = heptane or Xe) data suggests that the difference in rate of decay between $M(\eta^5\text{-}C_5H_5)(CO)_3(L)$ and $M(\eta^5\text{-}C_9H_7)(CO)_3(L)$ (M = Nb or Ta; L = heptane, N_2 or H_2) can only be explained in part by steric contributions, since we would expect a pentaphenylcyclopentadienyl group to exert a greater steric influence than an indenyl group. Therefore, the present study indicates that there is a subtle balance between the steric influence and the contribution by decay *via* a ring-slipped intermediate, with both factors playing a part in the increased reactivity of the indenyl complexes compared to the cyclopentadienyl complexes.

Conclusion

In this paper we have characterised the complexes $MCp'(CO)_3(X)$ (Cp′ = Cp or indenyl; M = Nb or Ta; X = *n*-heptane, H_2 or N_2) using step-scan FTIR. We have compared their reactivity using diode-laser based TRIR spectroscopy and have shown that the $M(\eta^5\text{-}C_9H_7)(CO)_3(n\text{-heptane})$ complexes are *ca*. an order of magnitude more reactive towards CO, H_2 or N_2 than the corresponding cyclopentadienyl complexes. Additionally, $M(\eta^5\text{-}C_9H_7)(CO)_3(N_2)$ are *ca*. 20–30 times more reactive than $MCp(CO)_3(N_2)$ and $Nb(\eta^5\text{-}C_9H_7)(CO)_3(\eta^2\text{-}H_2)$ is *ca*. 30 times more reactive than $NbCp(CO)_3(\eta^2\text{-}H_2)$. Although we were unable to compare the lifetimes of $Ta(\eta^5\text{-}C_9H_7)(CO)_3H_2$ and $TaCp(CO)_3H_2$ using our TRIR apparatus, our previous polymer experiments[34] have shown that the reactivities of these dihydride complexes follow the trends observed in this paper.

Experimental

The Nottingham laser based TRIR apparatus has been described in detail elsewhere.[43] In these experiments two different types of TRIR instrumentation were used, both employing a pulsed Nd:YAG laser (Quanta-Ray GCR-12, *ca*. 7 ns, 355 nm) to initiate photochemical reactions. We used either a step-scan FTIR interferometer (Nicolet Magna 860) or a continuous wave IR diode laser (Mütek MDS 1100) to monitor the transient IR absorptions. A full account of the experimental apparatus used for time-resolved step-scan FTIR measurements is given elsewhere.[44] Briefly, the apparatus comprises of a commercially available step-scan FTIR spectrometer (Nicolet Magna 860) equipped with a 100 MHz 12-bit digitizer and a 50 MHz MCT detector interfaced to the Nd:YAG laser. Synchronisation of the Nd:YAG laser with data collection was achieved using a pulse generator (Stanford DG535). A commercially available IR cell (Harrick, 0.5 mm) was used with a home built flow system. All characterisations were made using the step-scan apparatus. Once the IR band positions of the transient species were known, the IR diode system was used to obtain the kinetic measurements.

$NbCp(CO)_4$ **1**, $TaCp(CO)_4$ **2**, $Nb(\eta^5\text{-}C_9H_7)(CO)_4$ **3** and $Ta(\eta^5\text{-}C_9H_7)(CO)_4$ **4** were prepared using a literature procedure.[29] Hydrogen (Air Products), nitrogen (Air Products) and carbon monoxide (Air Products, Premier Grade) were used as supplied without further purification. *n*-Heptane (Aldrich, HPLC Grade) was distilled over CaH_2 prior to use. The solubilities[45,46] of CO, H_2 and N_2 in *n*-heptane were taken to be 1.2×10^{-2}, 0.45×10^{-2} and 0.95×10^{-2} M respectively. For the TRIR experiments the concentrations of solutions used were 5×10^{-4} M. All experiments were carried out at 298 ± 2 K.

Acknowledgements

We are grateful to the University of Nottingham for funding and Professor M. Poliakoff and Professor J. J. Turner for their helpful discussions. We thank Mr M. Guyler and Mr K. Stanley for their technical support.

References and notes

1 R. H. Crabtree, *Chem. Rev.*, 1985, **85**, 245.
2 D. M. Heinekey and W. J. Oldham, *Chem. Rev.*, 1993, **93**, 913.
3 M. A. Esteruelas and L. A. Oro, *Chem. Rev.*, 1998, **98**, 577.

4 G. J. Kubas, R. R. Ryan, B. I. Swanson, P. J. Vergamini and H. J. Wasserman, *J. Am. Chem. Soc.*, 1984, **106**, 451.
5 R. R. Eady and G. J. Leigh, *J. Chem. Soc.*, *Dalton Trans.*, 1994, 2739.
6 M. Hidai and Y. Mizobe, *Chem. Rev.*, 1995, **95**, 1115.
7 J. K. Burdett, A. J. Downs, G. P. Gaskill, M. A. Graham, J. J. Turner and R. F. Turner, *Inorg. Chem.*, 1978, **17**, 523.
8 R. L. Sweany, *J. Am. Chem. Soc.*, 1985, **107**, 2374.
9 R. L. Sweany, *J. Am. Chem. Soc.*, 1986, **108**, 6986.
10 R. L. Sweany, *Organometallics*, 1986, **5**, 387.
11 G. A. Ozin and J. Garciaprieto, *J. Am. Chem. Soc.*, 1986, **108**, 3099.
12 R. K. Upmacis, G. E. Gadd, M. Poliakoff, M. B. Simpson, J. J. Turner, R. Whyman and A. F. Simpson, *J. Chem. Soc.*, *Chem. Commun.*, 1985, 27.
13 R. K. Upmacis, M. Poliakoff and J. J. Turner, *J. Am. Chem. Soc.*, 1986, **108**, 3645.
14 G. E. Gadd, R. K. Upmacis, M. Poliakoff and J. J. Turner, *J. Am. Chem. Soc.*, 1986, **108**, 2547.
15 S. A. Jackson, R. K. Upmacis, M. Poliakoff, J. J. Turner, J. K. Burdett and F. W. Grevels, *J. Chem. Soc.*, *Chem. Commun.*, 1987, 678.
16 S. M. Howdle and M. Poliakoff, *J. Chem. Soc.*, *Chem. Commun.*, 1989, 1099.
17 S. M. Howdle, M. A. Healy and M. Poliakoff, *J. Am. Chem. Soc.*, 1990, **112**, 4804.
18 S. P. Church, F. W. Grevels, H. Hermann and K. Schaffner, *J. Chem. Soc.*, *Chem. Commun.*, 1985, 30.
19 S. A. Jackson, P. M. Hodges, M. Poliakoff, J. J. Turner and F. W. Grevels, *J. Am. Chem. Soc.*, 1990, **112**, 1221.
20 P. M. Hodges, S. A. Jackson, J. Jacke, M. Poliakoff, J. J. Turner and F. W. Grevels, *J. Am. Chem. Soc.*, 1990, **112**, 1234.
21 A. A. Bengali, R. G. Bergman and C. B. Moore, *J. Am. Chem. Soc.*, 1995, **117**, 3879.
22 C. Hall and R. N. Perutz, *Chem. Rev.*, 1996, **96**, 3125.
23 F. P. A. Johnson, M. W. George, V. N. Bagratashvili, L. N. Vereshchagina and M. Poliakoff, *Mendeleev Commun.*, 1991, **1**, 26.
24 B. S. Creaven, M. W. George, A. G. Ginzburg, C. Hughes, J. M. Kelly, C. Long, I. M. McGrath and M. T. Pryce, *Organometallics*, 1993, **12**, 3127.
25 C. J. Breheny, J. M. Kelly, C. Long, S. Okeefe, M. T. Pryce, G. Russell and M. M. Walsh, *Organometallics*, 1998, **17**, 3690.
26 G. I. Childs, C. S. Colley, J. Dyer, D. C. Grills, X.-Z. Sun, J. Yang and M. W. George, *J. Chem. Soc.*, *Dalton Trans.*, 2000, 4300.
27 R. B. Hitam and A. J. Rest, *Organometallics*, 1989, **8**, 1598.
28 A. J. Rest, M. Herberhold and M. Schrepfermann, *Organometallics*, 1992, **11**, 3646.
29 T. E. Bitterwolf, S. Gallagher, J. T. Bays, B. Scallorn, A. L. Rheingold, I. A. Guzei, L. LiableSands and J. C. Linehan, *J. Organomet. Chem.*, 1998, **557**, 77.
30 P. T. Snee, H. Yang, K. T. Kotz, C. K. Payne and C. B. Harris, *J. Phys. Chem. A*, 1999, **103**, 10426.
31 M. T. Haward, M. W. George, S. M. Howdle and M. Poliakoff, *J. Chem. Soc.*, *Chem. Commun.*, 1990, 913.
32 M. T. Haward, M. W. George, P. Hamley and M. Poliakoff, *J. Chem. Soc.*, *Chem. Commun.*, 1991, 1101.
33 M. W. George, M. T. Haward, P. A. Hamley, C. Hughes, F. P. A. Johnson, V. K. Popov and M. Poliakoff, *J. Am. Chem. Soc.*, 1993, **115**, 2286.
34 G. I. Childs, S. Gallagher, T. E. Bitterwolf and M. W. George, *J. Chem. Soc.*, *Dalton Trans.*, 2000, 4354.
35 K. L. McFarlane, B. Lee, W. F. Fu, R. vanEldik and P. C. Ford, *Organometallics*, 1998, **17**, 1826.
36 M. E. Rerek, L. N. Ji and F. Basolo, *J. Chem. Soc.*, *Chem. Commun.*, 1983, 1208.
37 R. H. Crabtree and D. G. Hamilton, *J. Am. Chem. Soc.*, 1986, **108**, 3124.
38 The previously reported values of k_{CO} were slightly higher than these (see ref. 32). The earlier values were calculated by measuring k_{obs} at only one concentration of CO and using the relationship $k_{obs} = k_{CO}[CO] + k_{Ar}$ to obtain k_{CO}, where k_{Ar} is the observed rate constant in the absence of added CO. We have repeated the determination of these values by using a more accurate method in which k_{obs} is measured at a series of CO concentrations and k_{CO} is obtained from the slope of the resulting plot.
39 G. I. Childs, D. C. Grills, X. Z. Sun and M. W. George, *Pure Appl. Chem.*, 2001, in press.
40 D. C. Grills, G. I. Childs and M. W. George, *Chem. Commun.*, 2000, 1841.
41 D. C. Grills, X. Z. Sun, G. I. Childs and M. W. George, *J. Phys. Chem. A*, 2000, **104**, 4300.
42 D. C. Grills, Ph.D. Thesis, University of Nottingham, 1999.
43 M. W. George, M. Poliakoff and J. J. Turner, *Analyst* (*London*), 1994, **119**, 551.
44 X.-Z. Sun, S. M. Nikiforov, J. Yang, C. S. Colley and M. W. George, *Appl. Spectrosc.*, 2001, submitted.
45 *IUPAC Solubility Data Series*, Pergamon Press, Oxford, 1990, vol. 43.
46 J. Makranczy, K. Begyery-Balog, L. Rusz and L. Patyi, *Hung. J. Ind. Chem.*, 1976, **4**, 269.